Laser-Induced Fluorescence of the CHClCHO Radical and Reaction of Oxygen Atoms with Halogenated Ethylenes

Satoshi Inomata, Isabelle Bridier, Masashi Furubayashi, Takashi Imamura, and Gen Inoue

Division of Atmospheric Environment, The National Institute for Environmental Studies, 16-2 Onogawa, Tsukuba, Ibaraki 305-0053, Japan

Makoto Yamaguchi

Institute of Research Innovation, 1201 Takada, Kashiwa, Chiba 277-0861, Japan

Nobuaki Washida*

Department of Chemistry, Graduate School of Science, Kyoto University, Sakyo-ku, Kyoto 606-8502, Japan

Received: April 3, 2001

A new laser-induced fluorescence spectrum has been observed in the region 320−360 nm. Since this spectrum is observed when reacting oxygen atoms with chlorinated ethylenes such as CH_2CHCl, CH_2CCl_2, CHClCHCl, and CHClCHF and also when chlorine atoms react with chloroacetaldehyde, the fluorescing molecules are identified as *cis*- and *trans*-2 chlorovinoxy radicals (*cis*- and *trans*-CHClCHO). From an analysis of the laser-induced single vibronic level fluorescence, some of the vibrational frequencies can be assigned for the ground electronic state ($\tilde{X}\ ^2A''$): ν_3(CO str) = 1567, ν_4(CH rock.) = 1380, ν_5(CH rock.) = 1309, ν_6(CC str) = 1060, ν_7(CCl str) = 820, ν_8(CCO bend.) = 677, and ν_9(CCCl bend.) = 220 cm^{-1} for *cis*-CHClCHO; ν_3 = 1581, ν_4 = 1379, ν_5 = 1267, ν_6 = 1145, ν_7 = 942, ν_8 = 472, and ν_9 = 324 cm^{-1} for *trans*-CHClCHO. Some of the vibrational frequencies for the excited $\tilde{B}^2A''$ state also are assigned. These vibrational assignments are supported by ab initio calculations. The calculated geometries of the *cis*- and *trans*-CHClCHO radicals are planar in the ground state and slightly nonplanar in the excited state. Radiative lifetimes of the excited *cis*- and *trans*-CHClCHO radicals are also reported. The experimental results showed that the C−C−O skeleton and spectroscopic character of the *cis*- and *trans*-CHClCHO are closer to those of CH_2CHO than to those of CH_2CFO. The mechanisms of the O + halogenated ethylene reactions are discussed.

Introduction

Recently, the formation of the 1-fluorovinoxy radical (CH_2-CFO) was observed by laser-induced fluorescence (LIF) when atomic oxygen, $O(^3P)$, reacted with several fluorinated ethylenes.[1−3] More recently, methyl-substituted vinoxy radicals[4] were observed in reactions of olefins with atomic oxygen. In the present study, a new LIF spectrum observed when reacting oxygen atoms with chlorinated ethylenes has been assigned to the 2-chlorovinoxy radical (CHClCHO). The spectroscopy of this radical is of interest because it was previously observed[1] that the 1-fluorovionxy radical has a tight carbonyl structure (C−C═O); i.e., the vibrational frequency of the C−O stretch in CH_2CFO, 1724 cm^{-1}, is much larger than that in CH_2CHO, 1540 cm^{-1}.[5]

It is known[6] that interaction of a ground state oxygen atom with an olefin or a substituted olefin may lead to any of the following three types of chemical change: (1) "abstraction" of an H atom by the O atom; (2) "addition" of the O atom to the olefin; and (3) "replacement" of an H atom or substituent (Cl atom in the present study) by the O atom. Since "replacement" itself is initially an "addition", followed by subsequent or simultaneous fragmentation of the resulting adduct, the structure of the resulting vinoxy radicals should give information about the site of the O atom attack on the halogenated ethylene double bond.

In the present paper, the generation and analysis of the new spectrum is desired, the rationale for assigning this spectrum to *cis*- and *trans*-2-CHClCHO is presented, and finally, mechanisms of the reactions of halogenated ethylenes with atomic oxygen are discussed.

Experimental Section

The apparatus used was the same as that described previously[1−4] and is only reviewed briefly here. The 2-chlorovinoxy radical was generated by reacting several chlorinated ethylenes with atomic oxygen, which was produced in a microwave discharge (2450 MHz) of an oxygen−helium mixture (10% O_2). Oxygen atoms and chlorinated ethylenes were mixed coaxially about 10 cm upstream of the detection area.

Fluorescence was induced by a frequency-doubled tunable dye laser (Lumonics HD-300) pumped by a Nd:YAG laser (Lumonics HYAG-750) for the range 355−344 and 336−308 nm and a Lambda Physik FL-3002E tunable dye laser pumped by a XeCl excimer laser (Questek 2440) to cover the range from 346 to 335 nm. Fluorescence was collected at right angles relative to the collinear counterpropagating laser beams and was measured with a Hamamatsu R268 photomultiplier tube using band-pass filters (L38 + B390, transmiting the range 360−500 nm).

The probe laser beam was perpendicular to the gas flow. The probe laser line width was 0.2 cm^{-1}. Dispersed fluorescence

10.1021/jp011253x CCC: $20.00
Published on Web 07/25/2001

spectra were recorded by pumping a particular vibrational transition with the probe laser frequency fixed, collecting the LIF through a lens and focusing it onto a 0.25 m monochromator (Nikon P-250). The resolution of this system was ~0.4 nm.

In a few experiments, LIF spectra were investigated by photolysis or by chlorine atom reactions. The appropriate precursor molecules (chlorinated acetaldehydes) were photolyzed by an ArF excimer laser (Lumonics EX-700). For chlorine atom reactions, radicals were produced by reacting precursor molecules with atomic chlorine, which was generated by the photolysis of CCl_4 at 193 nm.

$$CCl_4 + h\nu(193\ \text{nm}) \rightarrow Cl + CCl_3 \quad (1a)$$

$$\rightarrow 2Cl + CCl_2 \quad (1b)$$

All experiments were carried out at room temperature (296 ± 4 K). The chemicals were purchased from the following suppliers and used without further purification: CH_2=CHCl (99.9%, Takachiho); CH_2=CCl_2 (99%), *trans*-CHCl=CHCl (99%), *cis*-CHCl=CHCl (99%), CH_2ClCHO (40% in water), $(-CH_2CClO)_2$ (95%) (all from Toko Kasei); CCl_4 (98%), CH_3-CClO (98%) (both from Wako Pure Chemicals); CFCl=CH_2 (97%), CHCl=CHF (97%) (both from PCR); and CDCl=CDCl (cis/trans mixture, 99.8%, C/D/N Isotopes).

Results

1. Excitation Spectra. Figure 1a shows the LIF excitation spectrum observed in the region 323−357 nm when vinyl chloride (CH_2=CHCl) reacted with atomic oxygen. Part of this spectrum, which is shaded in Figure 1a, is identical to the spectrum of the vinoxy radical (CH_2CHO) reported previously.[5] The remainder of this spectrum is attributed to a new radical, which is thought to be the 2-chlorovinoxy radicals (CHClCHO) formed by reaction 2b or the 1-chlorovinoxy radicals (CH_2-CClO) formed by reaction 2c.

$$CH_2{=}CHCl + O(^3P) \rightarrow CH_2CHO + Cl \quad (2a)$$

$$\rightarrow CHClCHO + H \quad (2b)$$

$$\rightarrow CH_2CClO + H \quad (2c)$$

The LIF spectrum observed in the reaction of 1,1-dichloroethylene (CH_2=CCl_2) with atomic oxygen is shown in Figure 1b. The spectrum obtained is identical to the residual one shown in Figure 1a. The same spectrum as shown in Figure 1b was also observed when 1,2-dichloroethylene (CHCl=CHCl) reacted with atomic oxygen (not shown in Figure 1). The CHClCHO or CH_2CClO radicals could be produced by reactions 3 and 4.

$$CH_2{=}CCl_2 + O(^3P) \rightarrow CHClCHO + Cl \quad (3a)$$

$$\rightarrow CH_2CClO + Cl \quad (3b)$$

$$CHCl{=}CHCl + O(^3P) \rightarrow CHClCHO + Cl \quad (4a)$$

$$\rightarrow CH_2CClO + Cl \quad (4b)$$

As expected, no other LIF signals from vinoxy radicals were observed in these reaction systems. For reaction 3a to occur, the migration of a hydrogen atom in the hot adduct would be required; this will be discussed later.

A spectrum identical to that in Figure 1a was obtained when chloroacetaldehyde (CH_2ClCHO) reacted with atomic chlorine (Figure 1c). In this case, the CH_2ClCHO/CCl_4/He mixture was photolyzed by an ArF (193 nm) excimer laser. Since only the LIF spectrum of vinoxy radicals (shaded in Figure 1c) was observed by direct photolysis of CH_2ClCHO in the absence of CCl_4, reaction 5a, it was concluded that the 2-chlorovinoxy radical was produced by reaction 6a.

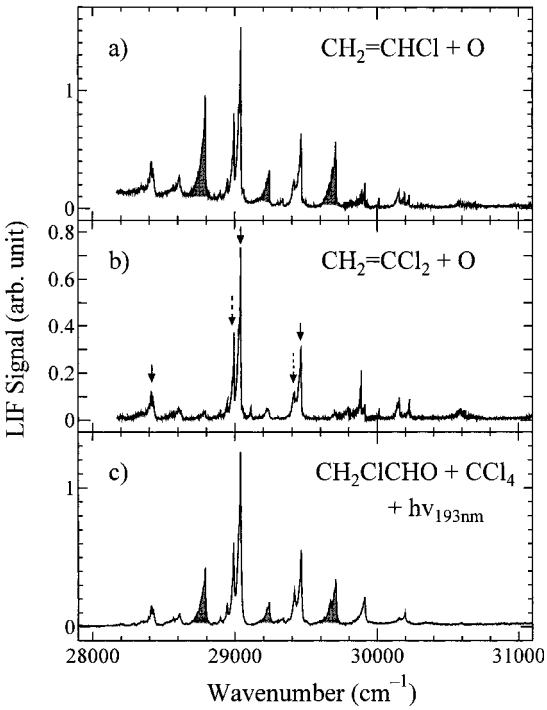

Figure 1. (a) Excitation spectrum of radicals produced in the CH_2-CHCl + $O(^3P)$ reaction. The shaded bands are from vinoxy (C_2H_3O) radicals. The residual spectrum is attributed to a new radical. The fluorescence intensity is normalized for laser power. The spectral resolution is 1 cm^{-1}. The pressures of CH_2CHCl, $O(^3P)$, and He are 1.5 mTorr, 2.0 mTorr, and 4 Torr, respectively. (b) LIF excitation spectrum of the new radical produced in the CH_2CCl_2 + $O(^3P)$ reaction. The pressures of CH_2CCl_2, $O(^3P)$, and He are 1.5 mTorr, 2.0 mTorr, and 4 Torr, respectively. For peaks shown by arrows, dispersed fluorescence spectra were measured (see the text). (c) LIF excitation spectrum of radicals produced in the photolysis of the CH_2ClCHO/CCl_4/He system at 193 nm (1 mJ/cm^2). The shaded bands are from the vinoxy radical, which is produced by the direct photolysis of CH_2-ClCHO. The residual spectrum is attributed to the new radical that is produced in the CH_2ClCHO + Cl reaction. The pressures of CH_2-ClCHO, CCl_4, and He are 0.3 mTorr, 50 mTorr, and 4 Torr, respectively.

$$CH_2ClCHO + h\nu(193\ \text{nm}) \rightarrow CH_2CHO + Cl \quad (5a)$$

$$\rightarrow \text{other products} \quad (5b)$$

$$CH_2ClCHO + Cl \rightarrow CHClCHO + HCl \quad (6a)$$

$$\rightarrow \text{other products} \quad (6b)$$

Consequently, the new LIF spectra in Figure 1 can be attributed to the 2-chlorovinoxy radical (CHClCHO), since the 1-chlorovinoxy radical (CH_2CClO) cannot be produced by reaction 6.

This assignment is consistent with the results that no LIF spectra were observed in the reaction of acetyl chloride (CH_3-CClO) with atomic chlorine and also after the photolyses of acetyl chloride or succinyl chloride ($ClCOCH_2CH_2COCl$). In these reactions, only the CH_2CClO radical should be produced.

$$CH_3CClO + Cl \rightarrow CH_2CClO + HCl \quad (7)$$

$$CH_3CClO + h\nu \rightarrow CH_2CClO + H \quad (8a)$$

$$\rightarrow \text{other products} \quad (8b)$$

$$(CH_2CClO)_2 + h\nu(193\ \text{nm}) \rightarrow 2CH_2CClO \quad (9a)$$

$$\rightarrow \text{other products} \quad (9b)$$

It might seem strange that the LIF spectrum of the CH_2CClO radical could not be observed since the LIF spectrum of the CH_2CFO radical has been observed in previous studies.[1−3] This is explored in more detail later.

The LIF spectrum of CHClCHO was also observed in the reaction of 1-chloro-2-fluoroethylene with atomic oxygen but could not be observed in the reaction of 1-chloro-1-fluoroethylene with oxygen atoms (only the LIF of CH_2CFO was observed). The former reaction can produce three different vinoxy-type radicals.

$$CHCl{=}CHF + O(^3P) \rightarrow CHClCHO + F \quad (10a)$$

$$\rightarrow CH_2CFO + Cl \quad (10b)$$

$$\rightarrow CHClCFO + H \quad (10c)$$

The present findings concerning the reactions forming (and not forming) vinoxy-type radicals are summarized in Table 1.

2. Equilibrium Structures and Fundamental Frequencies of Chlorovinoxy Radicals by ab Initio Calculation. Ab initio calculations were performed with the Gaussian 98 W program[7] using a 6-31 G* basis set. Optimized geometries of the ground ($\tilde{X}^2A''$) and excited $\tilde{B}^2A''$ state for the *cis*-CHClCHO, *trans*-CHClCHO, and CH_2CClO radicals were calculated by the CASSCF method as described previously.[8] Vibrational frequencies at optimized geometries were obtained from analytically calculated force constant matrices.

The geometries of the ground and excited $\tilde{B}$ states for each radical were optimized, and the calculated equilibrium structures are shown in Figure 2. Planar structures were found to be the most stable for the ground state of each radical. Among the three radicals in their ground states, the CH_2CClO radical is the most stable, i.e., about 27 kJ mol^{-1} more stable than the *cis*- and *trans*-CHClCHO radicals. For the excited $\tilde{B}$ states, nonplanar structures were found to be the most stable for the *cis*- and *trans*-CHClCHO radicals. On the other hand, for the CH_2CClO radical, the equilibrium structure of the excited $\tilde{B}$ state is still planar, which is also the case for CH_2CFO.[1] For all three radicals, the C−Cl bond lengths, 1.7−1.8 Å, are longer than the C−F bond length (∼1.3 Å) of CH_2CFO.[3] The $\tilde{B} \leftrightarrow \tilde{X}$ electronic transition energy, T_e, of CH_2CClO is slightly higher than T_e values of *cis*- and *trans*-CHClCHO.

The 12 normal frequencies, ω, of *cis*-CHClCHO, *trans*-CHClCHO, and CH_2CClO calculated from the optimized geometries in both the ground and excited $\tilde{B}$ states are listed in Table 2. All values of ω in Table 2 are multiplied by 0.9. Since the frequencies of the vibrational fundamentals are evidently different for the ClCCO and CC(Cl)O skeletons, these results should be helpful in analyzing the dispersed spectra of the fluorescing molecule.

3. Wavelength-Resolved Emission Spectra and Vibrational Fundamentals of the *cis*- and *trans*-CHClCHO Radicals. Figure 3 shows the wavelength-resolved emission spectra corresponding to excitation at (a) 29 040, (b) 29 466, and (c) 28 412 cm^{-1} (shown in Figure 1b by solid arrows). For excitation at 29 040 cm^{-1}, which is the strongest peak in Figure 1b, the main progression in emission has a spacing of 1580−1490 cm^{-1}, as shown in Figure 3a. This spacing should correspond to the C−O stretching mode (ν_3) in the ground state of the radical. Note in Figure 2 that for all three radicals, only the C−O bond distance has a large change between the ground and excited states; this should result in a long progression in the C−O stretch. Also the observed spacing is close to the predictions for ν_3 in Table 2. Six small peaks starting from each ν_3 peak of the main progression are apparent at intervals of ∼300, ∼480, ∼930, ∼1140, ∼1270, and ∼1380 cm^{-1}, as shown in Figure 3a. These are assigned to the ν_9(CCCl bend.), ν_8(CCO bend.), ν_7(CCl str), ν_6(CC str), ν_5(CH rock.), and ν_4(CH rock.) vibrational modes of *trans*-CHClCHO in the ground state. The most cogent reason for assigning the fluorescing radical to *trans*-CHClCHO is the appearance of a progression with a spacing of 480 cm^{-1}, which is attributed to the ν_8 vibrational mode of the *trans*-CHClCHO radical (449 cm^{-1} by ab initio calculation). Since most of the vibrational modes of a′ symmetry (from ν_1 to ν_9) in the ground state of *trans*-CHClCHO appeared on excitation at 29 040 cm^{-1}, the peak at 29 040 cm^{-1} in Figure 1a can be assigned to the 0_0^0 band for the $\tilde{X} \rightarrow \tilde{B}$ transition of *trans*-CHClCHO.

The dispersed fluorescence spectrum was measured for excitation at 28 993 cm^{-1}, corresponding to the second strongest

TABLE 1: Reactions Forming (and Not Forming) Vinoxy Type Radicals[a]

	vinoxy type radical			
reaction	CHClCHO	CH_2CHO	CH_2CFO	other vinoxy type radicals
$CH_2{=}CHCl + O$	strong	strong	−	−
$CH_2{=}CCl_2 + O$	strong	−	−	−
$CHCl{=}CHCl + O$	strong	−	−	−
$CHCl{=}CCl_2 + O$	−	−	−	−
$CHCl{=}CHF + O$	strong	−	weak	CHClCFO (strong)[b]
$CH_2{=}CClF + O$	−	−	strong	−
$CH_3CClO + h\nu_{193}$	−	−	−	−
$CH_3CClO + Cl$	−	−	−	−
$CH_2ClCHO + h\nu_{193}$	−	strong	−	−
$CH_2ClCHO + Cl$	strong	−	−	−
$(CH_2CClO)_2 + h\nu_{193}$	−	−	−	−
$CH_2{=}CHF + O$[c]	−	strong	strong	−
$CH_2{=}CF_2 + O$[c]	−	−	strong	−
$CHF{=}CHF + O$[b]	−	−	−	CHFCFO (strong)[b]
$CH_3CFO + h\nu_{193}$[d]	−	−	strong	−

[a] Key: strong, weak, and − represent "observed strongly", "observed weakly", and "not observed", respectively. [b] Reference 2. [c] Reference 1. [d] Reference 3.

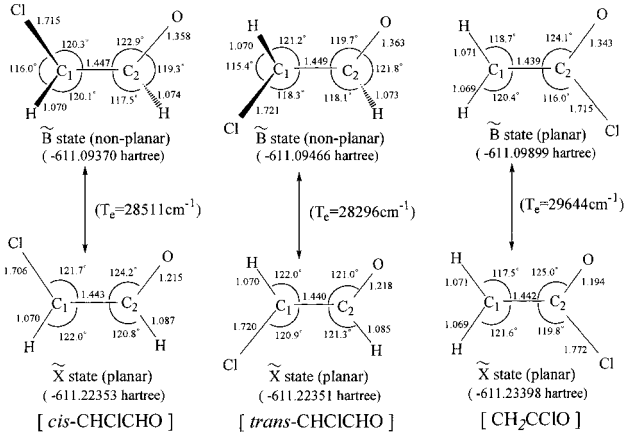

Figure 2. Equilibrium structures of the ground and excited $\tilde{B}$ states of the *cis*- and *trans*-CHClCHO and CH_2CClO radicals calculated by the ab initio method. Bond lengths are in angstroms, and bond angles are in degrees.

TABLE 2: Calculated Frequencies of Vibrational Fundamentals for *trans*- and *cis*-CHClCHO and CH_2CClO in Both the Ground and Excited State (Units in cm^{-1})

	cis-CHClCHO		*trans*-CHClCHO			CH_2CClO	
notation and vibr mode	ground state	excited $\tilde{B}$ state	ground state	excited $\tilde{B}$ state	notation and vibr mode	ground state	excited $\tilde{B}$ state
T_e	0	28511	0	28296		0	29644
ω_1(C_1H str)	3094	3092	3105	3094	ω_1($C_1H_1H_2$ asym. str)	3154	3152
ω_2(C_2H str)	2918	3050	2942	3068	ω_2($C_1H_1H_2$ sym. str)	3039	3047
ω_3(C_2O str)	1543	1701	1532	1677	ω_3(C_2O str)	1614	1733
ω_4(C_2H rock.)	1382	1318	1389	1284	ω_4($C_1H_1H_2$ sciss)	1432	1416
ω_5(C_1H rock.)	1309	1267	1236	1212	ω_5(C_1C_2 str)	1123	1148
ω_6(C_1C_2 str)	1032	1005	1081	1086	ω_6($C_1H_1H_2$ rock.)	992	954
ω_7(C_1Cl str)	782	770	859	836	ω_7(C_2Cl str)	617	649
ω_8(C_1C_2O bend.)	641	598	449	399	ω_8(C_1C_2O bend.)	453	406
ω_9(C_2C_1Cl bend.)	211	200	267	256	ω_9(C_1C_2Cl bend.)	350	341
ω_{10}(C_2H oop)	869	427	873	620	ω_{10}(wag. ip)	581	301
ω_{11}(C_1H oop)	426	395	485	444	ω_{11}(wag. oop)	496	121
ω_{12}(C_1C_2 torsion)	260	162	157	110	ω_{12}(C_1C_2 torsion)	328	294

[a] For the planar structure, the $\omega_1-\omega_9$ modes have a′ symmetry and the $\omega_{10}-\omega_{12}$ modes have a″ symmetry. All ab initio frequencies (ω) in Table 2 are multiplied by 0.9.

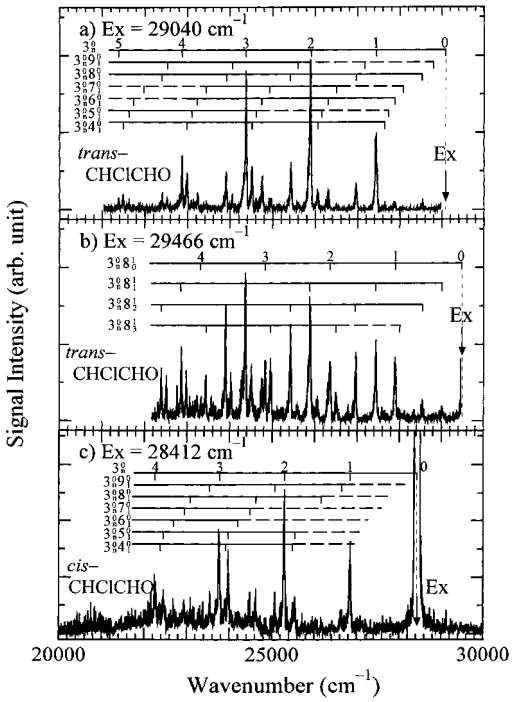

Figure 3. (a) Fluorescence spectrum of the *trans*-CHClCHO radical following excitation at 29 040 cm^{-1} (the 0_0^0 band) in the CHClCHCl + $O(^3P)$ reaction system. The pressures of CHClCHCl, $O(^3P)$, and He are 3 mTorr, 2 mTorr, and 4 Torr, respectively. The spectral resolution is 0.4 nm. (b) Fluorescence spectrum of the *trans*-CHClCHO radical following excitation at 29 466 cm^{-1} (the 8_0^1 band). Conditions are the same as those in (a). (c) Fluorescence spectrum of the *cis*-CHClCHO radical following excitation at 28 412 cm^{-1} (the 0_0^0 band). Conditions are the same as those in (a).

peak and appearing as a side peak of the 29 040 cm^{-1} peak (shown by a dashed arrow in Figure 1b). The fluorescence spectrum observed (not shown in Figure 3) was similar to the spectrum shown in Figure 3a, but all the spectral peaks were shifted to the red and the spectral profiles of each peak appeared slightly broader than those for 29 040 cm^{-1} excitation. The broadening of each peak is caused by the appearance of side peaks due to hot bands. Consequently, the peak at 28 993 cm^{-1} is probably a hot band, such as 12_1^1. The assignment of hot bands is discussed later.

Figure 3b shows the fluorescence spectrum for excitation at 29 466 cm^{-1}. In this case, the ν_8 progressions (spacing is about 480 cm^{-1}) coupled with the ν_3 vibrational mode are prominent.

TABLE 3: Observed Electronic Transition Energies and Frequencies of Vibrational Fundamentals for *trans*- and *cis*-CHClCHO (Units in cm^{-1})

	cis-CHClCHO		*trans*-CHClCHO	
notation	ground state	excited $\tilde{B}$ state	ground state	excited $\tilde{B}$ state
T_0	0	28412	0	29040
ν_3(C−O str)	1567		1581	1550
ν_4(CH rock.)	[1380]		1379	1189
ν_5(CH rock.)	[1309]		[1267]	1116
ν_6(C−C str)	[1060]		1145	974
ν_7(C−Cl str)	[820]	811	[942]	873
ν_8(CCO bend.)	[677]		472	426
ν_9(CCCl bend.)	[220]	195	[324]	

[a] Bracketed values were obtained by averaging the combination bands (see the text and Tables 1S−5S).

Therefore, the peak at 29 466 cm^{-1} is assigned to the 8_0^1 transition of the *trans*-CHClCHO radical. The dispersed fluorescence spectrum was also measured for excitation at the 29418 cm^{-1} peak, which seems to be a side peak of the 29 466 cm^{-1} peak (shown by a dashed arrow in Figure 1b). The fluorescence spectrum was similar to the spectrum shown in Figure 3b except for the broadening and small red shift of each band peak. Therefore, the peak at 29418 cm^{-1} is probably also a hot band such as $8_0^1 12_1^1$.

The dispersed fluorescence spectrum measured with excitation at 28 412 cm^{-1} is shown in Figure 3c. In this case, the main progression has a spacing of 1570−1500 cm^{-1}. Again this spacing should also correspond to the C−O stretching (ν_3) mode in the ground state of the CHClCHO radical. Six peaks starting from each ν_3 peak are apparent at intervals of ∼220, ∼680, ∼820, ∼1050, ∼1300, and ∼1390 cm^{-1}. These are different from the intervals observed for the *trans*-CHClCHO radical, so they are assigned to the ν_9, ν_8, ν_7, ν_6, ν_5, and ν_4 vibrational modes of the *cis*-CHClCHO radical in the ground state. Since these frequencies are in good agreement with the calculated vibrational fundamentals of *cis*-CHClCHO shown in Table 2, the peak at 28 412 cm^{-1} can be assigned to the 0_0^0 band for the $\tilde{X} \rightarrow \tilde{B}$ transition of the *cis*-CHClCHO radical.

The fluorescence bands and assignments for excitations at 28 992, 29 040, 29 418, 29 466, and 28 412 cm^{-1} are listed in Tables 1S−5S, respectively. From the vibrational energy spacings in Tables 1S−5S, the vibrational fundamentals in the ground state for the *cis*- and *trans*-CHClCHO radicals can be calculated. These are summarized in Table 3. Values for $\nu_4-\nu_9$ of *cis*-CHClCHO and ν_5, ν_7, and ν_9 of *trans*-CHClCHO in the

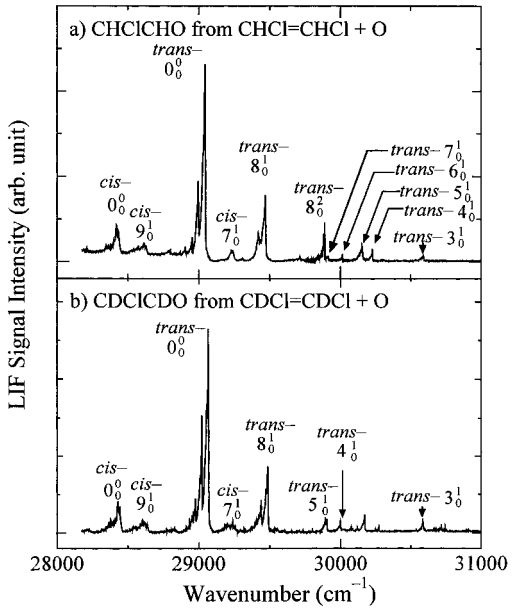

Figure 4. Laser-induced fluorescence excitation spectra of the CHClCHO and CDClCDO radicals. The fluorescence intensity is normalized for laser power. The spectral resolution is 1 cm^{-1}. (a) LIF spectrum of the CHClCHO radical produced in the CHClCHCl + O (^{3}P) reaction. (b) LIF spectrum of the CDClCDO radical produced in the CDClCDCl + O(^{3}P) reaction. The pressures of CHClCHCl or CDClCDCl, O(^{3}P), and He are 3 mTorr, 2 mTorr, and 4 Torr, respectively.

TABLE 4: Assignment of Observed Fluorescence Excitation Bands of *trans*- and *cis*-CHClCHO

wavenumber of peak (cm^{-1})	rel intens	assignment: *cis*-CHClCHO	assignment: *trans*-CHClCHO (hot band)	fundamental vibr freq (cm^{-1})
28 412	14	0^0_0		T_0(cis) = 28412
28 607	5	9^1_0		ν_9'(cis) = 195
28 898	6		(12^3_3)	
28 947	10		(12^2_2)	
28 992	40		(12^1_1)	
29 040	100	0^0_0		T_0(trans) = 29040
29 223	5	7^1_0		ν_7'(cis) = 811
29 418	14		$(8^1_0 12^1_1)$	
29 466	34	8^1_0		ν_8'(trans) = 426
29 888	19	8^2_0		
29 913	3	7^1_0		ν_7'(trans) = 873
30 014	3	6^1_0		ν_6'(trans) = 974
30 156	8	5^1_0		ν_5'(trans) = 1116
30 229	7	4^1_0		ν_4'(trans) = 1189
30 590	2	3^1_0		ν_3'(trans) = 1550

ground state are calculated by averaging over several values obtained from the combination bands shown in Tables 1S−5S. These values are given in brackets in Table 3.

The observed vibrational fundamentals in the ground state for *cis*- and *trans*-CHClCHO in Table 3 are in reasonable agreement with the values calculated by the ab initio method in Table 2. The agreement is much better for *cis*- and *trans*-CHClCHO than for CH_2CClO. The results again support the proposal that the fluorescing molecules are *cis*- and *trans*-CHClCHO, and not CH_2CClO.

4. Assignment of the Excitation Spectrum. Since the 0^0_0 band for the *cis*- and *trans*-CHClCHO radicals were identified from the fluorescence spectra, other peaks in the excitation spectrum can be assigned, guided by the calculated vibration frequencies in the excited $\tilde{B}$ state in Table 2. These assignments are shown in Figure 4a, and all of the results are listed in Table 4.

TABLE 5: Assignment of Observed Fluorescence Excitation Bands of CDClCDO

wavenumber (cm^{-1})	rel intens	assignment: *cis*-CDClCDO	assignment: *trans*-CDClCDO (hot band)	fundamental vibr freq (cm^{-1})
28 427	15	0^0_0		T_0(cis) = 28427
28 621	5	9^1_0		ν_9'(cis) = 194
28 936	6		(12^3_3)	
28 977	18		(12^2_2)	
29 021	58		(12^1_1)	
29 068	100	0^0_0		T_0(trans) = 29068
29 242	6	7^1_0		ν_7'(cis) = 819
29 439	17		$(8^1_0 12^1_1)$	
29 487	34	8^1_0		ν_8'(trans) = 419
29 910	7	5^1_0		ν_5'(trans) = 842
30 007	6	4^1_0		ν_4'(trans) = 939
30 589	6	3^1_0		ν_3'(trans) = 1521

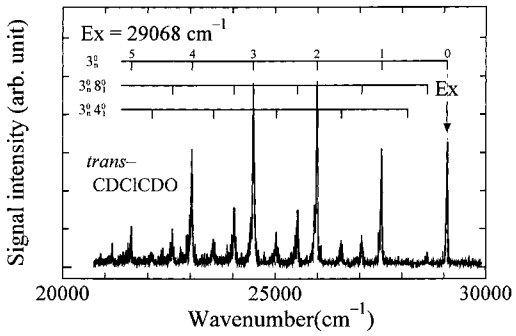

Figure 5. Fluorescence spectrum of the *trans*-CDClCDO radical following excitation at 29 068 cm^{-1} (the 0^0_0 band) in the CDClCDCl + O(^{3}P) reaction system. The pressures of CDClCDCl, O(^{3}P), and He are 2.1 mTorr, 1.2 mTorr, and 3.2 Torr, respectively.

The electronic transition energies (T_0) and vibrational fundamentals for *cis*- and *trans*-CHClCHO in the excited $\tilde{B}$ state are summarized in Table 3. Values are in good agreement with the calculated values by ab initio method (Table 2).

5. Isotope Shift. Figure 4b shows the LIF excitation spectrum of the CDClCDO radical observed when 1,2-dichloroethylene-1,2-d_2 (CDCl═CDCl) reacted with atomic oxygen.

$$CDCl{=}CDCl + O(^3P) \rightarrow CDClCDO + Cl \qquad (11)$$

The spectrum of CDClCDO is similar to that of CHClCHO except for small isotope shifts. Since the assignments for the excitation spectrum of CHClCHO were made in Figure 4a and Table 4, the assignments could be extended to CDClCDO radical. These assignments are shown in Figure 4b, and all of the results are listed in Table 5. As shown in Table 5, the electronic transition energies (T_0) for the $\tilde{X} \rightarrow \tilde{B}$ transition of *cis*- and *trans*-CDClCDO are 28 427 and 29 068 cm^{-1}, respectively. These values are slightly (15 and 28 cm^{-1}, respectively) higher than those for *cis*- and *trans*-CHClCHO. Some of the fundamental vibrational frequencies could be assigned for the excited $\tilde{B}$ state: $\nu_7' = 819$ and $\nu_9' = 194$ cm^{-1} for *cis*-CDClCDO; $\nu_3' = 1521$, $\nu_4' = 939$, $\nu_5' = 842$, and $\nu_8' = 419$ cm^{-1} for *trans*-CDClCDO.

Figure 5 shows the wavelength-resolved emission spectrum corresponding to excitation at the 0^0_0 band of the *trans*-CDClCDO radical (29 068 cm^{-1}). Progressions of 3^0_n, $3^0_n 8^0_1$, and $3^0_n 4^0_1$ are clearly evident. From the intervals of these progressions, the frequencies of the vibrational fundamentals for ν_3'', ν_4'', and ν_8'' for ground state *trans*-CDClCDO were calculated as 1568, 965, and 481 cm^{-1}, respectively. The dispersed fluorescence spectrum was also measured with the excitation at 29 487 cm^{-1}. The fluorescence bands and assign-

TABLE 6: Isotope Shift of Electronic Transition Energies and Frequencies of Vibrational Fundamentals between CHClCHO and CDClCDO (Units in cm^{-1})

	ab initio calc				obsd in the present study			
	cis-2-chloro-vinoxy		*trans*-2-chloro inoxy		*cis*-2-chloro-vinoxy		*trans*-2-chloro-vinoxy	
	$\tilde{X}$	$\tilde{B}$	$\tilde{X}$	$\tilde{B}$	$\tilde{X}$	$\tilde{B}$	$\tilde{X}$	$\tilde{B}$
T_0					0	24	0	38
ν_3(C−O str)	−25	−19	−27	−26			−13	−29
ν_4(CH rock.)	−379	−375	−508	−377			−414	−250
ν_5(CH rock.)	−548	−510	−278	−311				−274
ν_6(C−C str)	176	140	105	−2				
ν_7(C−Cl str)	−38	−46	−101	−83		4		
ν_8(CCO bend.)	−29	−21	−6	8			−5	−7
ν_9(CCCl bend.)	−1	−6	−16	−15		0		

[a] Shift represents the frequency difference between CDClCDO and CHClCHO, {ν(CDClCDO) − ν(CHClCHO)}.

ments are summarized in Tables 6S (29 068 cm^{-1} excitation) and 7S (29 487 cm^{-1} excitation).

The isotope shifts of the observed vibrational fundamentals between CDClCDO and CHClCHO ($\nu_{CDClCDO} - \nu_{CHClCHO}$) and these obtained from ab initio calculations are listed in Table 6. In ab initio calculations, the normal frequencies for CDClCDO were calculated by using the same geometry as CHClCHO (Figure 2), changing only the mass of the two hydrogen atoms (calculations were carried out by using the same force constant matrix). The isotope shifts observed are in good agreement with those calculated. The isotope shifts for the vibrational modes of ν_4 and ν_5 (both are CH rock.) are large and those of the ClCCO skeleton are small in both the ground and excited states.

Calculations of the isotope effect between ^{35}Cl and ^{37}Cl in the CHClCHO radical were carried out by the ab initio method. The isotope shifts for all vibrational modes were very small. Even for the C−Cl stretching mode (ν_7) of the *trans*-CHClCHO radical, the shift was only 4 cm^{-1} in both the ground and excited states and for other vibrational modes, shifts were less than 2 cm^{-1}.

6. Anharmonicity of the ν_3 Vibration in the Ground State and Radiative Lifetimes. The vibrational spacings for the ν_3 mode in the ground states of the *cis*-CHClCHO, *trans*-CHClCHO, and *trans*-CDClCDO radicals are $\nu_3''(0-1)$ = 1567, $\nu_3''(1-2)$ = 1558, $\nu_3''(2-3)$ = 1538, and $\nu_3''(3-4)$ = 1499 cm^{-1} for *cis*-CHClCHO, $\nu_3''(0-1)$ = 1581, $\nu_3''(1-2)$ = 1559, $\nu_3''(2-3)$ = 1516, $\nu_3''(3-4)$ = 1504, and $\nu_3''(4-5)$ = 1489 cm^{-1} for *trans*-CHClCHO, and $\nu_3''(0-1)$ = 1568, $\nu_3''(1-2)$ = 1514, $\nu_3''(2-3)$ = 1516, $\nu_3''(3-4)$ = 1447, and $\nu_3''(4-5)$ = 1418 cm^{-1} for *trans*-CDClCDO (see Tables 1S, 2S, 5S, and 6S). These spacings can be fitted to eq 12 using a diatomic approximation.

$$G(v+1) - G(v) = \omega_e - 2\omega_e x_e(v+1) \qquad (12)$$

From the least-squares fitting, values of ω_e and $\omega_e x_e$ were calculated to be 1596.5 and 11.2 cm^{-1} for *cis*-CHClCHO, 1601.5 and 11.95 cm^{-1} for *trans*-CHClCHO, and 1602.7 and 18.35 cm^{-1} for *trans*-CDClCDO, respectively. The energies of each C−O stretching vibrational state of the ground states *cis*-CHClCHO, *trans*-CHClCHO, and *trans*-CDClCDO are given by

$$G(v_3)_{cis-CHClCHO} = 1596.5\left(v_3+\frac{1}{2}\right) - 11.2\left(v_3+\frac{1}{2}\right)^2 \qquad (13)$$

$$G(v_3)_{trans-CHClCHO} = 1601.5\left(v_3+\frac{1}{2}\right) - 12.0\left(v_3+\frac{1}{2}\right)^2 \qquad (14)$$

$$G(v_3)_{trans-CDClCDO} = 1602.7\left(v_3+\frac{1}{2}\right) - 18.35\left(v_3+\frac{1}{2}\right)^2 \qquad (15)$$

The fluorescence lifetimes of the *cis*- and *trans*-CHClCHO radicals in the $\tilde{B}$ state were measured by observing the time profile of the fluorescence, which showed an exponential decay. The radiative lifetimes measured by excitation of several peaks in the excitation spectrum (Figure 4) are summarized in Table 7. The radiative lifetimes of the *cis*- and *trans*-CHClCHO radicals (100−200 ns) are longer than those of the CH_2CFO radical (50−80 ns) and close to those of vinoxy (CH_2CHO) radicals (100−150 ns).

Discussion

1. Hot Bands Analysis. As already described, several bands of the excitation spectrum of the CHClCHO radical shown in Figure 1 consist of closely spaced peaks. These satellite peaks can be assigned to hot bands. Figure 6 shows the expanded band profile around the 0_0^0 band of the *trans*-CHClCHO radical. The main progression has a spacing of about 47 cm^{-1}. This spacing is attributed to the difference between the frequency of the ν_{12}'' mode of the ground state and that of the excited $\tilde{B}$ state of the *trans*-CHClCHO radical (this value is 47 cm^{-1} by ab initio calculations, as shown in Table 2). Therefore, the 28 993, 28 947, and 28 898 cm^{-1} peaks are assigned to the 12_1^1, 12_2^2, and 12_3^3 bands, respectively. The observed relative intensities of the 0_0^0, 12_1^1, 12_2^2, and 12_3^3 bands ($I(0_0^0)$:$I(12_1^1)$:$I(12_2^2)$:$I(12_3^3)$ = 100:40:10:6) are in good agreement with the relative populations of the ν_{12} vibrational levels in the ground state calculated for a Boltzmann distribution at 298 K ($N(\nu''=0)$:$N(\nu_{12}''=1)$:$N(\nu_{12}''=2)$:$N(\nu_{12}''=3)$ = 100:43:19:8) assuming that the spacing of each vibrational level of the ν_{12} mode is constant ($\Delta\nu_{12}''$ = 174 cm^{-1} from Table 2).

Two small peaks (at 29 028 and 28 993 cm^{-1}) starting from the 0_0^0 and 12_1^1 bands are apparent at an interval of about 13 cm^{-1}. These might also be hot bands of the ν_9 vibrational mode. These peaks are assigned to the 9_1^1 and $9_1^1 12_1^1$ bands of the *trans*-CHClCHO radical (by the ab initio calculations in Table 2, the interval is 12 cm^{-1}). In this case, the relative populations of the ground state ν_9 levels calculated by the Boltzmann distribution at 298 K are $N(\nu_9''=0)$:$N(\nu_9''=1)$ = 100:24, assuming the value of $\Delta\nu_9''$ is 297 cm^{-1}.

Similarly, the peak at 29 418 cm^{-1}, which seems to be a side peak of the 8_0^1 band (29 466 cm^{-1}) is assigned to the $8_0^1 12_1^1$ band. The above assignments are listed in Table 4 as hot bands.

Figure 7 shows the expanded (24 000−26 500 cm^{-1} region) band profile of the wavelength-resolved emission spectra of the *trans*-CHClCHO radical corresponding to excitation at (a) 29 040 cm^{-1} (the 0_0^0 excitation) and (b) 28 992 cm^{-1} (the 12_1^1 hot band excitation). In Figure 7b, the combination bands of the 12_1^1 vibrational mode appear strongly in addition to the band peaks appearing in Figure 7a. Thus, all peaks appear to be twin peaks. The spacings of these twin peaks are 40−50 cm^{-1}, which corresponds to the difference between the frequency of the ν_{12} mode in the ground (157 cm^{-1} in Table 2) and the excited $\tilde{B}$ state (110 cm^{-1} in Table 2). The results are consistent with the excitation spectrum shown in Figure 6.

2. Comparison with the CH_2CHO and CH_2CFO Radicals. It is interesting to compare the spectroscopic data for *cis*-CHClCHO, *trans*-CHClCHO, CH_2CFO, and CH_2CHO radicals, as summarized in Table 8.

The geometries of the ground state CH_2CHO,[10−13] CH_2CXO, *cis*-CHXCHO, and *trans*-CHXCHO (X = F and Cl) radicals

TABLE 7: Fluorescence Lifetimes of the Excited B State of *cis*- and *trans*-CHClCHO

ν_{ex} (cm^{-1})	assignment	lifetime (ns)
	(a) *cis*-CHClCHO	
28 412	0^0_0	199 ± 8
28 607	9^1_0	195 ± 9
29 223	7^1_0	143 ± 13
	(b) *trans*-CHClCHO	
29 040	0^0_0	135 ± 6
29 466	8^1_0	115 ± 10
29 913	7^1_0	113 ± 19

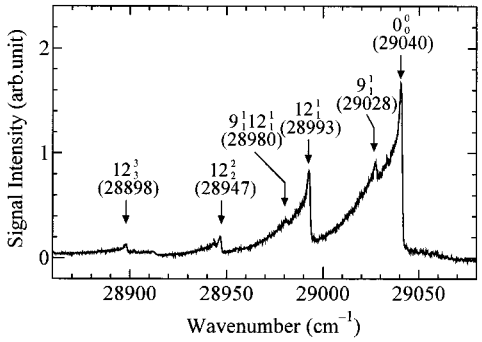

Figure 6. Expanded band profile around the 0^0_0 band of the *trans*-CHClCHO radical. The CHClCHO radical was produced in the $CH_2CCl_2 + O(^3P)$ reaction. The pressures of CH_2CCl_2, $O(^3P)$, and He are 1.6 mTorr, 2.0 mTorr, and 3.0 Torr, respectively. Spectral resolution is 0.2 cm^{-1}.

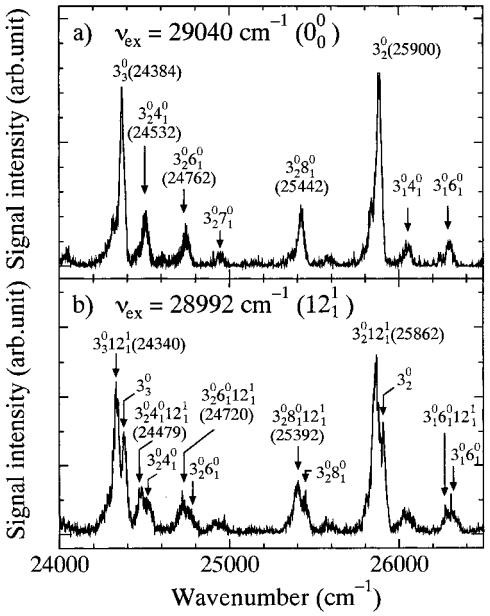

Figure 7. Expanded band profiles of the dispersed fluorescence spectra of the *trans*-CHClCHO radical in the 24 000−26 500 cm^{-1} region. (a) Excitation at 29 040 cm^{-1} (the 0^0_0 band), (b) Excitation at 28 992 cm^{-1} (the 12^1_1 band). Experimental conditions are same as those in Figure 6. Spectral resolution is 0.4 nm. Numbers in parentheses show wavenumbers of the peak position.

optimized by ab initio calculations are all planar. On the other hand, the geometries of the *cis*- and *trans*-CHXCHO in the excited $\tilde{B}$ state are nonplanar, whereas those of the CH_2CHO[13−16] and CH_2CXO radicals are planar. This can be explained by valence bond pictures of the *trans*-CHClCHO and CH_2CClO radicals. As illustrated in Figure 8, an electron on a chlorine at the 2-position is donated to the π orbital of the vinoxy in the excited $\tilde{B}$ state. For the *trans*-CHClCHO, the localized electron density on the 2-position carbon induces the pyramidalization

TABLE 8: Comparison of the Spectroscopic Data of *cis*-CHClCHO, *trans*-CHClCHO, CH_2CFO, and CH_2CHO Radicals

	cis-CHClCHO[a]	*trans*-CHClCHO[a]	CH_2CFO[b]	CH_2CHO[c]
structure $\tilde{X}$	planar	planar	planar	planar
$\tilde{B}$	nonplanar	nonplanar	planar	planar
$T_0(\tilde{X} \rightarrow \tilde{B})$ (cm^{-1})	28 412	29 040	29 874	28 786
vibr fundamentals ($\tilde{X}$, cm^{-1})				
CO (str)	1567	1581	1724	1543
CC (str)	1060	1145	847	957
CCO (bend.)	677	472	416	500
vibr fundamentals ($\tilde{B}$, cm^{-1})				
CO (str)		1550	1790	1621
CC (str)		974	874	917
CCO (bend.)		426	421	449
fluorescence lifetime of the 0^0_0 band (ns)	199	135	81	190
isotope shift of T_0 by D	+24	+38	−7[d]	+42[e]

[a] This work. [b] Reference 1. [c] Reference 9. [d] Reference 3. [e] Reference 5.

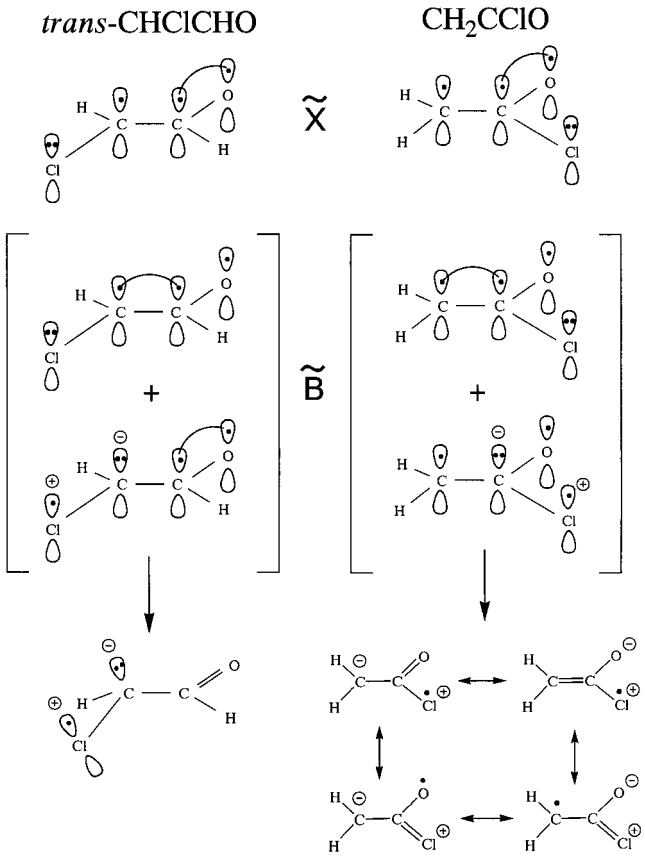

Figure 8. Valence bond pictures of the *trans*-CHClCHO and CH_2CClO radicals.

due to sp^3 hybridization. For CH_2CClO, a resonance structure is formed, and the planar structure is retained in the $\tilde{B}$ state. This explanation is in good agreement with the change of the C−Cl bond length in the $\tilde{X} \rightarrow \tilde{B}$ transition shown in Figure 2. The C−Cl bond length of the CH_2CClO is shortened in the excited $\tilde{B}$ state, while that of the *trans*-CHClCHO does not change.

The observed electronic transition ($\tilde{X} \rightarrow \tilde{B}$) energies, T_0, of the *cis*- and *trans*-CHClCHO radicals (28 412 and 29 040 cm^{-1}, respectively) are closer to that of CH_2CHO (28 786 cm^{-1}) than to that of CH_2CFO (29 874 cm^{-1}). The ground state fundamental frequencies of the C−O stretching vibration of *cis*- and *trans*-

CHClCHO (1567 and 1581 cm^{-1}, respectively) are slightly larger than that of CH_2CHO (1543 cm^{-1}) but considerably smaller than that of CH_2CFO (1724 cm^{-1}). This means that the C—C—O skeleton of the *cis*- and *trans*-CHClCHO radicals does not have a tight carbonyl structure like the CH_2CFO radical (C—C═O).[1] The ground state fundamental frequencies of the C—C stretching vibration are larger in *cis*- and *trans*-CHClCHO (1060 and 1145 cm^{-1}, respectively) than in CH_2CFO (847 cm^{-1}) and CH_2CHO (957 cm^{-1}). This means that a chlorine atom at the 2-position makes the C—C bond slightly stronger. The fundamental frequency of the CCO bending is larger in *cis*-CHClCHO (ν_8 = 677 cm^{-1}) than in *trans*-CHClCHO (ν_8'' = 472 cm^{-1}). This might be caused by the repulsion force between the lone-pair electrons of the chlorine and oxygen atoms. Indeed, the CCO angle of *cis*-CHClCHO (122.9°) is larger than that of *trans*-CHClCHO (119.7°), (Figure 2).

The radiative lifetimes of the 0_0^0 band for the $\tilde{B} \rightarrow \tilde{X}$ transition of *cis*- and *trans*-CHClCHO are closer to that for CH_2-CHO than for CH_2CFO. The $\tilde{X} \rightarrow \tilde{B}$ electronic transition energy, T_0, for *cis*- and *trans*-CDClCDO are slightly higher than for *cis*- and *trans*-CHClCHO. This isotope shift is also similar to those of CH_2CHO and CD_2CDO.[5]

On the whole, the molecular characteristics of the *cis*- and *trans*-CHClCHO radicals are closer to those of CH_2CHO than to those of CH_2CFO.

3. Reaction Mechanisms for Reactions of Halogenated Ethylene with O(^{3}P). Three puzzling results appear in the present study. (1) In reactions of oxygen atoms with chlorinated ethylenes, only the 2-chlorovinoxy radical (*cis*- and *trans*-CHClCHO) could be observed, while the 1-chlorovinoxy radical (CH_2CClO) was not observed by LIF. This raises a question; was the CH_2CClO radical produced in the O + chloroethylene reactions or not? (2) On the other hand, in reactions of oxygen atoms with fluorinated ethylenes, only the 1-fluorovinoxy radical (CH_2CFO) was observed,[1] while the 2-fluorovinoxy radical (CHFCHO) was not observed. Why was the CHFCHO radical not observed? (3) The formation of CHClCHO radicals was observed in the $CH_2 = CCl_2 + O(^3P)$ reaction, reaction 3a. The CHClCHO radical cannot be produced without hydrogen and/or chlorine atom migration in the O-adduct. By what mechanism is the CHClCHO produced?

In general, it is known[6,17−20] that interaction of a ground state oxygen atom, O(^{3}P), with an olefin may lead to any of the following three types of chemical change: (1) "abstraction" of an H atom from the olefin by the O atom, (2) "addition" of the O atom to the olefin, and (3) "replacement" of a hydrogen atom or radical (halogen atom in this study) from the olefin by the O atom. "Replacement" is initially an addition combined with subsequent or simultaneous fragmentation of the resulting adduct. Results obtained in the present study are related to the replacement processes.

Cvetanovic[17] suggested that the initial step of the addition reaction consists of an attachment of the electrophilic O atom to the carbon atom of the double bond, forming a triplet biradical (ketocarbene). The O atom should attach itself to the less substituted carbon atom on ethylenes having electron-donating substituents such as methyl (or ethyl), because the electron density is higher on the less substituted carbon.[21,22] This prediction was verified in our previous work[4] on methyl-substituted vinoxy radicals. In the case of electron-withdrawing substituents such as halogens (especially fluorine), oxygen atoms should add to the halogen-substituted carbon atom. There is a barrier to the release of a hydrogen atom or a halogen atom, and the rate of release must compete with the rate of intersystem crossing. The vinoxy or substituted vinoxy radicals are thought to be produced by this direct release of a hydrogen atom or a halogen atom. If direct release does not occur, intersystem crossing occurs and a hydrogen atom migrates to the adjacent carbon atom, forming an energized singlet state aldehyde or ketone. (In this migration process, it has not been established whether halogen atoms are also capable of migration in the highly excited adduct.) The aldehyde or ketone dissociates unimolecularly by a C—C or C—X (X = H, or halogen) fission. In the following, the formation mechanism of halogenated vinoxy radicals (including the 1-fluorovinoxy radical of the previous study[1]) are discussed in accordance with the foregoing generalizations.

4. Fluorinated Vinoxy Radicals. In a previous study,[1] the 1-fluorovinoxy radical (CH_2CFO) was observed when oxygen atoms reacted with CH_2CHF, CH_2CF_2, or CH_2CFCl, but it could not be observed in the CHFCHF + O reaction (see Table 1). Moreover the LIF of the 2-fluorovinoxy radical (CHFCHO) could not be observed in any of these reaction systems, although it is not known whether the CHFCHO radical can emit fluorescence.

According to the generalization described above, (1) the O atom attaches to the fluorine-substituted carbon atom in the initial step and (2) direct release of an H atom or an F atom might compete, although a C—H bond has a slightly smaller bond energy than a C—F bond.

On the basis of these two assumptions, the formation mechanisms of CH_2CFO could be explained as follows:

$$CH_2{=}CHF + O \rightarrow {}^{\bullet}CH_2{-}C(O^{\bullet})HF \rightarrow CH_2CFO + H \quad (16a)$$

$$\rightarrow CH_2CHO + F \quad (16b)$$

$$CH_2{=}CF_2 + O \rightarrow {}^{\bullet}CH_2{-}C(O^{\bullet})F_2 \rightarrow CH_2CFO + F \quad (17)$$

$$CH_2{=}CFCl + O \rightarrow {}^{\bullet}CH_2{-}C(O^{\bullet})FCl \rightarrow CH_2CFO + Cl \quad (18)$$

$$CHF{=}CHF + O \rightarrow {}^{\bullet}CHF{-}C(O^{\bullet})HF \rightarrow CHFCFO + H \quad (19a)$$

$$\rightarrow CHFCHO + F \quad (19b)$$

In reaction 17, there is no competition between the release of an H and an F atoms. A Cl atom must be released in preference to an F atom in reaction 18, because a C—Cl bond is much weaker than a C—F bond. The formation of CHFCFO, reaction 19a, shown in Table 1 is also reasonable on the basis of the above model. The CHFCHO radical could not be observed by LIF in reactions 16−19. The only route capable of forming CHFCHO is reaction 19b, although it is uncertain whether reaction 19b can compete with reaction 19a.

5. Chlorinated Vinoxy Radicals. As shown in Table 1 and Figure 1b, the CHClCHO and CH_2CHO radicals were produced in the CH_2CHCl + O reaction. In this case, if O atoms added to the chlorine-substituted side of the vinyl chloride double bond, CH_2CHO was produced by reaction 2a.

$$CH_2{=}CHCl + O \rightarrow {}^{\bullet}CH_2{-}C(O^{\bullet})HCl \rightarrow CH_2CHO + Cl \quad (2a)$$

To form CHClCHO, O atoms must also add to the carbon at the 2-position.

$$CHCl{=}CH_2 + O \rightarrow {}^{\bullet}CHCl{-}C(O^{\bullet})H_2 \rightarrow CHClCHO + H \quad (2b)$$

This means that O atoms can add to either side of the vinyl chloride double bond.

Another possible route for forming the CH_2CHO radical involves C−Cl bond fission in a hot singlet chloroacetaldehyde (CH_2ClCHO), which could be formed by a 1,2-migration of an H or a Cl atom in a highly excited adduct (biradical) after intersystem crossing.

$$^{\bullet}CHCl{-}C(O^{\bullet})H_2 \xrightarrow{\text{(H-migration)}} CH_2ClCHO^* \rightarrow CH_2CHO + Cl \quad (20)$$

$$^{\bullet}CH_2{-}C(O^{\bullet})HCl \xrightarrow{\text{(Cl-migration)}} CH_2ClCHO^* \rightarrow CH_2CHO + Cl \quad (21)$$

Since a C−Cl bond has a much smaller bond energy than a C−H bond, C−Cl fission can compete with C−C fission. To determine in which process the CH_2CHO is formed, measurements of the pressure dependence of the yield of the CH_2CHO radical are necessary.

Only the LIF spectrum of CHClCHO was observed in the CH_2CCl_2 + O reaction. However, the 2-chlorovinoxy radical (CHClCHO) cannot be produced by direct replacement. Only the 1-chlorovinoxy radical (CH_2CClO) can be produced by a replacement process.

$$CH_2{=}CCl_2 + O \rightarrow {}^{\bullet}CH_2{-}C(O^{\bullet})Cl_2 \rightarrow CH_2CClO + Cl \quad (3b)$$

Although the LIF spectrum of CH_2CClO could not be observed, the CH_2CClO radical should be present in the CH_2CCl_2 + O reaction system. Probably, the CH_2CClO radical does not emit fluorescence because of predissociation. In the previous study,[1] it has been suggested that the CH_2CFO radical in the excited $\tilde{B}$ state is partially predissociated. Thus, the radiative lifetimes of CH_2CFO for the $\tilde{B} \rightarrow \tilde{X}$ transition are shorter than those of other vinoxy type radicals (Table 8). Thus, it is likely that the CH_2CClO radical predissociates in the excited $\tilde{B}$ state and so is not observed by LIF.

The formation of CHClCHO may be explained by the unimolecular decomposition of dichloroacetaldehyde following the O atom addition to the less chorine-substituted side of the double bond.

$$CCl_2{=}CH_2 + O \rightarrow {}^{\bullet}CCl_2{-}C(O^{\bullet})H_2 \xrightarrow{\text{(H-migration)}} CHCl_2CHO^* \rightarrow CHClCHO + Cl \quad (3a)$$

In the CHClCHCl + O reaction, the CHClCHO radical can be formed by the addition of an O atom to the double bond.

$$CHCl{=}CHCl + O \rightarrow {}^{\bullet}CHCl{-}C(O^{\bullet})HCl \rightarrow CHClCHO + Cl \quad (4a)$$

The CHClCHO from the CHClCHF + O reaction can be also explained by reaction 10a.

$$CHCl{=}CHF + O \rightarrow {}^{\bullet}CHCl{-}C(O^{\bullet})HF \rightarrow CHClCHO + F \quad (10a)$$

$$\rightarrow CHClCFO + H \quad (10c)$$

The weak LIF signal of CH_2CFO (see Table 1) might be formed by the H atom migration.

$$^{\bullet}CHCl{-}C(O^{\bullet})HF \xrightarrow{\text{(H-migration)}} CH_2ClCFO^* \rightarrow CH_2CFO + Cl \quad (10b)$$

As described above, the reaction mechanisms of the chlorinated ethylene are not as clear as the case of fluorinated ethylenes. It is not clear whether O atoms add to either side or only to the chlorine-substituted side of the double bond. Halogens are basically electron-withdrawing substituents. However, since the chlorine is less electronegative than the fluorine, an electron of a chlorine atom can be donated to the π orbital of the double bond; so-called "back-donation" occurs. Such back-donation has been reported as chemical shifts of olefinic compounds.[22] As illustrated in Figure 8, an electron release from a chlorine at the 2-position to the π orbital of vinoxy is a type of the electron back-donation. Therefore, to which side of the double bond O atoms add depends on the localized electron density. In other words, the chlorine does not act always as an electron-withdrawing substituent.

The mechanisms of the reactions of O + olefins and O + halogen-substituted olefins are basically similar, and these can be generalized by an attachment of the electrophilic O atom to the double bond, as suggested by Cvetanovic.[17]

Conclusion

(1) New laser-induced fluoresence bands were observed in the 320−360 nm region.

(2) The new spectrum could be observed in reactions of CH_2CHCl, CH_2CCl_2, CHClCHCl, and CHClCHF with atomic oxygen and also following chlorine atom reaction with CH_2ClCHO. The new bands are assigned to the *cis*- and *trans*-2-chlorovinoxy (CHClCHO) radicals.

(3) From an analysis of the fluorescence spectra, some of the vibrational fundamentals were determined. These assignments were confirmed by ab initio calculation on *cis*- and *trans*-CHClCHO. The structure of the C−C−O skeleton and spectroscopic character of *cis*- and *trans*-CHClCHO are closer to CH_2CHO than to CH_2CFO.

(4) The initial attack of oxygen atoms to fluorine- or chlorine-substituted ethylenes was discussed, and it was confirmed that the mechanisms of reactions of O + olefins and O + halogen-substituted olefins are basically similar and that reactions can be generalized by an attachment of the electrophilic O atom to the double bond, as suggested by Cvetanovic in 1963.

Acknowledgment. We thank Professor Kyle D. Bayes for his helpful suggestions and comments. The support for FY 1996−1998 of Japan Environment Agency and from the Grant-in-Aid for FY 1998−2000 of the Ministry of Education and Science is gratefully acknowledged. I.B. was a Japan Science and Technology Agency Fellow 1994−1996.

Supporting Information Available: Tables 1S−7S containing information on assignment of observed fluorescence bands of the *trans*-CHClCHO (1S−4S), *cis*-CHClCHO (5S), and *trans*-CDClCDO (6S and 7S) are available free of charge via the Internet at http//pubs.acs.org.

References and Notes

(1) Furubayashi, M.; Bridier, I.; Inomata, S.; Washida, N.; Yamashita, K. *J. Chem. Phys.* **1997**, *106*, 6302.

(2) Washida, N.; Furubayashi, M.; Imamura, T.; Bridier, I.; Miyoshi, A. *J. Chem. Phys.* **1997**, *107*, 6998.

(3) Inomata, S.; Furubayashi, M.; Imamura, T.; Washida, N.; Yamaguchi, M. *J. Chem. Phys.* **1999**, *111*, 6356.

(4) Washida, N.; Inomata, S.; Furubayashi, M. *J. Phys. Chem. A* **1998**, *102*, 7924.
(5) Inoue, G.; Akimoto, H. *J. Chem. Phys.* **1981**, *74*, 425.
(6) Cvetanovic, R. J. *J. Phys. Chem. Ref. Data* **1987**, *16*, 261.
(7) Frisch, M. J.; Trucks, G. W.; Schlegel, H. B.; Scuseria, G. E.; Robb, M. A.; Cheeseman, J. R.; Zakrzewski, V. G.; Montgomery, J. A.; Stratmann, R. E.; Burant, J. C.; Dapprich, S.; Millam, J. M.; Daniels, A. D.; Kudin, K. N.; Strain, M. C.; Farkas, O.; Tomasi, J.; Barone, V.; Cossi, M.; Cammi, R.; Mennucci, B.; Pomelli, C.; Adamo, C.; Clifford, S.; Ochterski, J.; Petersson, G. A.; Ayala, P. Y.; Cui, Q.; Morokuma, K.; Malick, D. K.; Rabuck, A. D.; Raghavachari, K.; Foresman, J. B.; Cioslowski, J.; Ortiz, J. V.; Stefanov, B. B.; Liu, G.; Liashenko, A.; Piskorz, P.; Komaromi, I.; Gomperts, R.; Martin, R. L.; Fox, D. J.; Keith, T.; Al-Laham, M. A.; Peng, C. Y.; Nanayakkara, A.; Johnson, G.; Chen, W.; Wong, M. W.; Andres, J. L.; Head-Gordon, M.; Replogle, E. S.; Pople, J. A. *Gaussian 98*, revision A.2; Gaussian, Inc.: Pittsburgh, PA, 1998.
(8) Yamaguchi, M.; Furubayashi, M.; Inomata, S.; Washida, N. *Chem. Phys. Lett.* **1998**, *298*, 93.
(9) Brock, L. R.; Rohlfing, E. A. *J. Chem. Phys.* **1997**, *106*, 10048.
(10) Baird, N. C.; Taylor, K. F. *Can. J. Chem.* **1979**, *58*, 733.
(11) Baird, N. C.; Gupta, R. R.; Taylor, K. F. *J. Am. Chem. Soc.* **1979**, *101*, 4531.
(12) Wetmore, R. W.; Schaefer, H. F., III; Hiberty, P. C.; Brauman, J. I. *J. Am. Chem. Soc.* **1980**, *102*, 5470.
(13) Yamaguchi, M.; Momose, T.; Shida, T. *J. Chem. Phys.* **1990**, *93*, 4211.
(14) Dupuis, M.; Wendoloski, J. J.; Lester, W. A., Jr. *J. Chem. Phys.* **1982**, *76*, 488.
(15) Huyser, E. S.; Feller, D.; Borden, W. T.; Davidson, E. R. *J. Am. Chem. Soc.* **1982**, *104*, 2956.
(16) Yamaguchi, M. *Chem. Phys. Lett.* **1994**, *221*, 531.
(17) Cvetanovic, R. J. *Advances in Photochemistry*; Wiley & Sons Interscience: New York, 1963; Vol. 1, pp 115.
(18) Cvetanovic, R. J.; Singleton, D. L. *Rev. Chem. Intermed.* **1984**, *5*, 183.
(19) Huie, R. E.; Herron, J. T. *Prog. React. Kinet.* **1975**, *8*, 1.
(20) Lin, M. C. *Adv. Chem. Phys.* **1980**, *42*, 113.
(21) Kajimoto, O.; Fueno, T. *Tetrahedron Lett.* **1972**, *32*, 3329.
(22) Kajimoto, O.; Fueno, T. *Chem. Lett.* **1972**, 103.